A Software Package to Simulate CCD Photometry: Application to High-Motion *K2* Observations

Nicholas Saunders [1,2], Rodrigo Luger [3,4], Rory Barnes [3,4]

ABSTRACT

We present `scope` (Simulated CCD Observations for Photometric Experimentation), a `python` package to create a forward model of telescope detectors and simulate stellar targets with motion relative to the CCD. The primary application of this package is the simulation of the *Kepler* Space Telescope detector to predict and characterize increased instrumental noise in the spacecraft's final campaigns of observation. As the fuel powering the spacecraft's stabilizing thrusters runs out and thruster fires begin to sputter or fail, stellar Point Spread Functions (PSFs) will experience more extreme and less predictable motion relative to regions of varied sensitivity on the spacecraft detector, generating more noise in transiting exoplanet light curves. Using our simulations, we demonstrate that current de-trending techniques effectively capture and remove systematics caused by sensitivity variation for spacecraft motion as high as about ten times that currently experienced by *K2*. The `scope` package is open-source has been generalized to allow custom detector and stellar target parameters. Future applications include simulating observations made by the Transiting Exoplanet Survey Satellite (*TESS*) and ground based observations with synthetic atmospheric interference as testbeds for noise-removal techniques.

1. Introduction

Despite the failure of two reaction wheels in 2012 and 2013, the *Kepler* Space Telescope has continued to produce valuable data in its new configuration, *K2*, with significantly higher precision than ground based telescopes (Howell et al. 2014). However, due to the

---

[1] NASA Ames Kepler/K2 Guest Observer Office, Mountain View, CA 94035

[2] nicholas.k.saunders@nasa.gov

[3] Department of Astronomy, University of Washington, Box 351580, Seattle, WA 98195, USA

[4] Virtual Planetary Laboratory, Seattle, WA 98195, USA

unstable pointing caused by the missing reaction wheels, targets have significant motion relative to the quantum sensitivity variation of the telescope detector, creating noise in *K2* light curves. A number of attempts have been made to isolate and remove the instrumental noise from *K2* data (Vanderburg & Johnson 2014; Armstrong et al. 2015; Lund et al. 2015; Huang et al. 2015; Aigrain et al. 2015, 2016). Through the application of data processing pipelines, namely the EPIC Variability Extraction and Removal for Exoplanet Science Targets (`EVEREST`) pipeline developed by Luger et al. (2016), the noise in *K2* light curves can be reduced to the level of the original *Kepler* mission for up to 15th magnitude (Luger et al. 2017).

However, as the *Kepler* Space Telescope runs out of fuel, its motion due to thruster fires is expected to become less predictable and the magnitude of targets' motion relative to the detector will increase. With higher motion, targets will traverse more regions of varied pixel sensitivity, contributing more noise to the light curves of *K2* targets. Eventually, when thruster fuel has been depleted entirely or the fuel level becomes too low for useful correction, the telescope may enter a phase of constant drift, at which point targets will traverse many pixels across the detector. This will also increase the likelihood of flux pollution from neighbors, as stellar PSFs may overlap over the course of a campaign.

In this paper, we present an approach to characterize increased noise due to high motion and assess noise-removal methods. §2 describes the mathematical methods of our simulation, §3 explores the results of our testing, §4 elaborates on future applications of this work, §5 provides usage examples, and §6 discusses our conclusions.

2. Methods

Effective removal of instrumental noise requires a thorough understanding of its source. Stellar motion relative to the pixel sensitivity variation on the *Kepler* CCD causes fluctuation in the amount of light recorded by the telescope detector over time. In order to accurately simulate the instrumental noise characteristic of *K2* light curves, it is necessary to generate a forward model for the pixel sensitivity variation of the CCD. Light curves that were simulated using this sensitivity variation model are adequate to serve as well-understood sample targets on which to determine noise levels resulting from light curves generated under conditions of high roll magnitude and apply de-trending methods. To accurately represent the *Kepler* CCD, we generated a model for the detector that included both inter-pixel sensitivity variation between pixels and intra-pixel sensitivity variation within each pixel.

2.1. PSF Model

A stellar PSF was generated with a characteristic two-dimensional Gaussian shape, which includes covariance between x and y dimensions to capture PSF distortion due to incident light aberration on the *Kepler* detector. We define our model for $F(t)$, the total flux received by the telescope detector as a function of time, to be

$$F(t) = \sum_{aperture} \iint_{pixel} [s(x,y)P(x,y)\tau(t)]dxdy, \tag{1}$$

where $s(x,y)$ is the sensitivity variation function, modeled by a low order polynomial, and $P(x,y)$ is the PSF of the star, centered at (x_0, y_0) with amplitude A. $\tau(t)$ is a simulated transit function. The pixel sensitivity model is given by the bivariate polynomial

$$s(x,y) = \sum_n a_{x,n} x^n a_{y,n} y^n, \tag{2}$$

with coefficients $a_{x,n}, a_{y,n}$ defined to result in a sensitivity map that peaks in the center of each pixel and falls off toward the edge. The PSF model is given by a sum over two-dimensional Gaussians

$$
\begin{aligned}
P(x,y) = A \sum_m \frac{1}{2\pi\sigma_{x,m}\sigma_{x,n}\sqrt{1-\rho_m^2}} \exp &\left[-\frac{1}{2(1-\rho_m^2)} \left(\frac{(x-x_{0,m})^2}{2\sigma_{x,m}^2} \right.\right. \\
&\left.\left. + \frac{(y-y_{0,m})^2}{2\sigma_{y,m}^2} - \frac{2\rho_m(x-x_{0,m})(y-y_{0,m})}{\sigma_{x,m}\sigma_{y,m}} \right) \right]
\end{aligned}
\tag{3}
$$

where σ_x, σ_y are the standard deviations of the PSF in x and y, and ρ is the correlation coefficient between x and y.

The coefficients $a_{x,n}, a_{y,n}$ were determined to emulate the magnitude of sensitivity variation on the *Kepler* CCD based on its contribution to the noise in *K2* light curves. Sensitivity coefficients are defined as independent in x and y for consistency with the Kepler Instrument Handbook (Van Cleve & Caldwell 2016). Our method for choosing values for sensitivity variation coefficients a_n is descried in the following section.

2.2. Pixel Sensitivity Variation

Our model for the sensitivity variation was chosen to emulate the same noise magnitude as real *K2* observations. For our noise metric, we use the Combined Differential Photometric Precision for consistency with Luger et al. (2016). We used a two-step benchmarking process

to estimate the magnitude of variation in quantum sensitivity and contribution by photon noise and background noise.

First we considered the no-motion case. For a large population of simulated targets with randomly generated stellar magnitude and detector position, the noise versus magnitude trend should closely follow that of the original *Kepler* mission. To most accurately capture the characteristics of *K2* data when analyzing the noise contributed by quantum sensitivity variation, our model included two sources of synthetic noise – photon noise and background noise – which contribute to the trend of increased noise for higher magnitude targets for the *Kepler* mission. Benchmark Test 1 serves to constrain the levels of injected photon noise and background noise. The test consisted of plotting the CDPP for 1,000 targets from the original *Kepler* mission and calculating the median value for each Kp Mag at intervals of 0.5.

We generated five synthetic light curves for each 0.5-Mag interval with the following random variation of PSF parameters: centroid position varied by up to 0.2 pixels in both x and y, σ_x and σ_y varied up to 10% ($\sim$0.05 pixels), and correlation coefficient ρ varied up to 40%. Each of these five simulated light curves is plotted against the *Kepler* noise trend. This test was run iteratively on varied values of both background and photon noise until the slopes of the two trends approximately corresponded. To see the comparative noise of the resultant simulation, see Figure 1.

In Benchmark Test 2, we consider the case of current *K2* motion. To accomplish this, we injected motion from 1,000 cadences of the *K2* target EPIC 205998445, creating a simulated example of a current observation to benchmark our model against *K2* data. EPIC 205998445 is a *K2* C03 star with $Kp = 12.029$ located $\sim$60% of the distance from the center of the detector plane to its edge. Statistics about the motion data used in our simulation can be found in Table 1. This star was chosen because it is an isolated 12th magnitude star, and the peak of the magnitude distribution for C03 was roughly 12. It is also located far enough from the center of the detector that it experiences significant motion during roll events, but not too near the edge that its motion is uncharacteristically high for *K2* targets.

To calculate motion, the column pixel correction (`POS_CORR1`) and row pixel correction (`POS_CORR2`), corresponding to motion in x and y respectively, were accessed from the target pixel file header. These offsets were added to the calculated centroid position of the simulated PSF for each cadence. Total magnitude of motion as reported in Table 1 represents the calculated maximum distance between centroid positions over the course of the simulated cadences.

With real *K2* motion applied, sensitivity variation parameters were adjusted until CDPP

versus Kp Mag corresponded to the trend of real $K2$ observations. Sensitivity variation was altered by adjusting the coefficients on the $s(x)s(y)$ polynomial model to achieve different drops in sensitivity from pixels' centers to their edges, as well as adjusting the random variation in sensitivity between pixels. We found that a stochastic distribution of sensitivity with up to 1% variation between pixels and 2.48% variation within pixels, from center to edge, resulted in Benchmark Test 2 following the most similar trend to the expected result. Our sensitivity polynomial went up to third order with coefficients {1, 0, -0.05}. The results of Benchmark Test 2 can be seen in Figure 2.

A sample detector with included sensitivity variation can be seen in Figure 3. The calculation used in our simulation does not generate the sensitivity model and PSF individually, and instead passes the parameters into a singly-integrated function. This saves a computational step and speeds up the process. However, we were unable to solve the second integral prior to calculation because the first integral of a Gaussian results in an error function, which is non-analytic.

For campaigns up to 17, stellar PSFs already traverse various regions of sensitivity variation on the CCD due to pointing instability. As spacecraft motion increases, PSFs will move more dramatically across many pixels, which will contribute significant noise to sputtering-$K2$ light curves. With a working model for sensitivity variation, we examined the high-motion case.

2.3. Increased Motion

To test how PLD performs on targets with high motion relative to the detector, we injected motion vectors with various coefficients into our synthetic models. A coefficient of 1 corresponds to typical $K2$ motion (maximum of ~ 0.59 pixels), while a coefficient of 10 results in motion of up to 5.85 pixels. More detail about the motion used in our simulations can be found in Table 1.

Our method to increase motion involved simply multiplying the pixel offset due to current $K2$ motion by constant coefficients. This ensured the target traversed more pixels over a wider range of the detector while keeping the position calculation simple enough to avoid introducing new opportunity for error. Because it is still unclear exactly how increased motion will manifest in the spacecraft's observations when fuel is expended, we opted to examine the simplest case of linearly increasing motion magnitude. It should be noted that this may not be the most appropriate treatment for all de-trending methods, particularly those that rely on fitting the centroid position of the target. However, the method used in

Coefficient	Motion (pix)	Max Motion (pix)	Motion (arcsec)	Max Motion (arcsec)
1	0.17 ± 0.12	0.59	0.67 ± 0.47	2.33
2	0.34 ± 0.24	1.17	1.34 ± 0.95	4.66
5	0.84 ± 0.59	2.93	3.34 ± 2.37	11.65
10	1.68 ± 1.19	5.85	6.68 ± 4.74	23.30

Table 1:: Coefficients applied to the motion vectors of *K2* target EPIC 205998445, an isolated C03 star. A coefficient of 1 corresponds to current motion, with each subsequent coefficient simply increasing the magnitude of motion by that factor. Motion is given in both pixels and arcseconds.

the EVEREST pipeline (pixel level decorrelation) is agnostic to centroid position and relies simply on the measured flux in each pixel, so our treatment of motion is thorough enough for the goal of testing noise-removal methods.

3. Results

With a robust forward model of *K2* established, including both motion and sensitivity variation, we were able to apply our de-trending methods to stars with various tiers of increased motion to predict and understand the results of thruster failure. To elaborate on the results of our test, we first introduce our de-trending methods (§3.1), and then examine the application of these methods to our simulated data (§3.2).

3.1. PLD

After generating a set of light curves representative of extreme motion *K2* observations, we tested systematics removal methods to assess the potential value of sputtering-*K2* data. To de-trend our synthetic light curves, we used a variant of the method applied in the EVEREST pipeline. EVEREST utilizes a method called pixel level decorrelation (PLD), developed by Deming et al. (2015) for the *Spitzer* Space Telescope.

PLD seeks to remove noise generated by intra-pixel sensitivity variation independent of apparent motion of the star. This method is particularly effective for *K2* light curves despite the magnitude of apparent motion being high, and EVEREST can recover *Kepler*-like precision in exoplanet light curves for targets up to $Kp = 15$. For a more detailed treatment of PLD, see the paper by Deming et al. (2015) and the first two EVEREST papers (Luger et al. 2016,

2017).

3.2. Motion Tests

For each motion coefficient, 5 simulated light curves were generated for magnitudes from Kp Mag= 10 to Kp Mag= 15.5 at 0.5-magnitude intervals. Each light curve was de-trended with 2nd order PLD, and the CDPP was calculated. The average CDPP of the 5 simulations was calculated and plotted as a function of Kp Mag. A detailed look at the results of our motion tests can be found in Figure 4.

Synthetic targets with 2x current $K2$ motion achieved $Kepler$-like photometry up to $Kp = 13$ when de-trended with 2nd order PLD, and noise levels remained below 200 ppm up to $Kp = 15$ (compared to < 100 ppm for $Kepler$). Noise in light curves of targets with 5x motion remained below 400 ppm up to $Kp = 15.5$. After de-trending with the EVEREST pipeline, we were able to retrieve transit parameters from simulated light curves with this magnitude of noise. This indicates that sustained observation during periods of increased spacecraft motion may result in the continued collection of valuable data.

These results were achieved by applying PLD to pixels within an aperture around our simulated stars. The aperture is defined to exclude extraneous background and photon noise in order to maximize light from our target. In applications for real targets, it is often necessary to also consider nearby bright stars when defining an aperture. scope includes the ability to add neighboring stars, however they were excluded from these tests for simplicity. Future consideration will be given to automating aperture definitions, particularly because high motion PSFs will traverse more pixels and will therefore have a higher likelihood of crowding.

4. Discussion

4.1. Direct Measurement of Sensitivity

We acknowledge the inconsistency in resultant intra-pixel sensitivity variation between our calibration tests and the direct measurement of the sub-pixel response by Vorobiev et al. (2018). Future work is necessary to identify the source of the meaningfully different conclusions, and we would like to identify a number of factors that likely contribute. The primary suspect is the degeneracy between inter- and intra-pixel sensitivity variation in our motion benchmark, both of which contribute to the systematic noise of synthetic light curves.

Also included in this degeneracy are the magnitudes of background noise and photon noise.

Our calibration was based on *K2* observations, and there are a number of physical differences between the current state of the space telescope detectors and the laboratory environment. Vorobiev et al. (2018) acknowledge the temperature difference, and when considered in combination with the potential degradation of the telescope detector after nearly a decade of use, this could result in a significant difference in measured sensitivity.

4.2. Future Applications

Due to the internal optics of the Transiting Exoplanet Survey Satellite (*TESS*), observed stellar PSFs may be large relative to the pixels on the CCD. In the instance that *TESS* also faces motion issues, there will be a significant need to test de-trending methods with an emphasis on defining ideal apertures. With a combination of large PSFs and increased noise, apertures and associated aperture-based PLD methods will be an essential piece of our noise-removal strategy for *TESS*.

Further, the space telescope's trajectory could cause a periodic variation in the incident sunlight on the telescope, which will affect the quantum sensitivity of pixels. Periodically changing sensitivity could cause *TESS* PSFs to "breathe" as the temperature rises and falls, and apertures around *TESS* targets will need to expand and contract correspondingly to effectively capture the desired stellar signal. Our forward model serves as an established simulation for cases of time-variable PSFs due to both motion and periodic sensitivity changes.

The stellar PSF parameters can be easily adjusted in the forward model produced by `scope` to cover more pixels and more accurately capture PSFs characteristic of *TESS* observations. Using this simulation, it would be valuable to test various apertures and motion cases prior to the first public release of observations.

Seeing aberration and atmospheric interference are additional sources of noise that could be included in the `scope` model. PLD was developed for *Spitzer* and modified for application to *K2*, but has seen little application elsewhere. For ground-based observations with significant noise due to pointing issues or atmospheric interference, PLD may be a valuable tool to make the most of data. `scope` is an ideal testbed for this type of noise-removal because it allows users to perform tests on noisy observations of synthetic sources that are well understood with input parameters that can be compared to post-processing results. Though it was initially imagined for space-based telescopes, this software has potentially useful applications for ground-based telescopes.

5. Using `scope`

All of our code is open-source and publicly available online. Our simulation package can be installed by running

```
pip install tele-scope
```

To create a light curve with `scope`, first instantiate a `Target` object:

```
import scope
star = scope.Target()
```

A light curve can be generated by calling the `GenerateLightCurve()` function, which returns an array of image files (`tpf`), a one-dimensional flux light curve (`flux`), and an array of matrices containing the error in each pixel (`ferr`):

```
tpf, flux, ferr = star.GenerateLightCurve()
```

After a target is created, transits, variability, or neighbors can be added with the following functions (with example parameters provided):

```
star.AddTransit(depth=.01, per=15, dur=.5, t0=5.)
star.AddVariability(var_amp=0.005, freq=0.25)
star.AddNeighbor(magdiff=1., dist=1.7)
```

Alternatively, a `Target` can be instantiated containing added features with default parameters by changing the following boolean parameters:

```
star = scope.Target(transit=True, variable=True, neighbor=True)
```

The detector with sensitivity variation can be displayed by calling

```
star.DisplayDetector()
```

To de-trend with second order PLD, run

```
star.Detrend()
```

Documentation and examples can be found online at nksaunders.github.io/scope. The code is publicly available at github.com/nksaunders/scope.

6.   Conclusions

We have created a forward model of the *Kepler* space telescope detector, `scope`, which includes inter- and intra-pixel sensitivity variation and mathematical simulations of stellar PSFs to test de-trending methods for exoplanet targets. Using these simulations, we have demonstrated that `EVEREST` and PLD are capable of reducing systematic noise to higher precision than ground based observations in *K2* light curves with up to 10x current spacecraft motion. We have shown that in the event of spacecraft thruster sputtering due to diminishing fuel reserves, valuable data can likely still be collected and analyzed to benefit *K2* science goals. The question surrounding the usefulness of high-motion data is increasingly relevant to making decisions about the future of *K2* observations, and our hope is to emphasize the potential value in continued observation and contribute to the de-trending of future data.

Though *TESS*, the successor to *Kepler*, has launched, there remains a wealth of both existing and unobserved *K2* data that offers valuable contribution to our understanding of exoplanetary systems. Earthlike exoplanets can be difficult to identify in the high-magnitude noise of current *K2* data, which will continue to get noisier as the mission reaches its conclusion. *TESS* and *JWST* will likely face their own challenges with data analysis and noise-removal, and the tools developed for *K2* will be foundations and references for new solutions. The methods we have presented aim to produce the most precise exoplanet identification, characterization, and analysis from the data we have available, and prepare for the next generation of space telescopes.
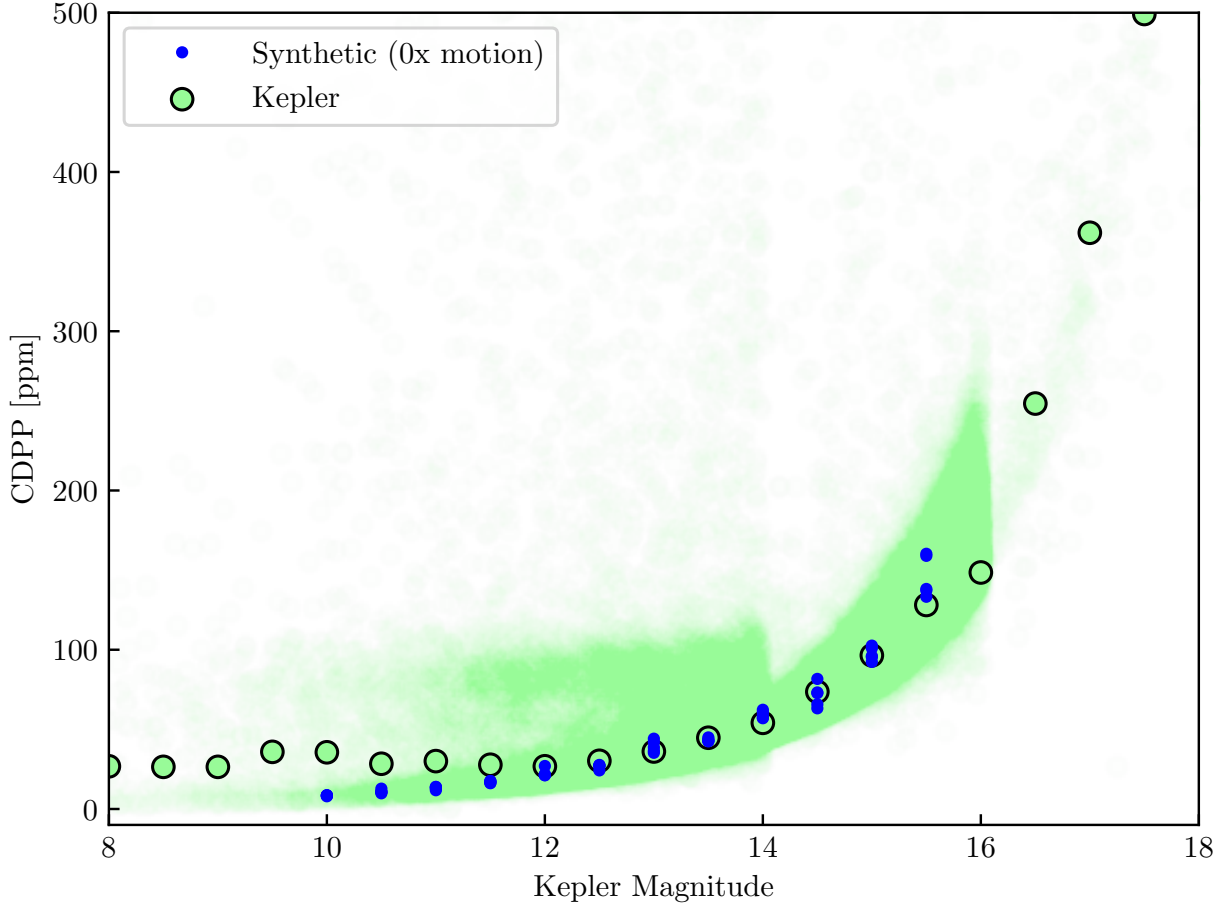
Fig. 1.— Benchmark Test 1: Noise level (CDPP) of our simulated light curves with no motion compared to original *Kepler* targets as a function of *Kp* Mag. The green trend demonstrates the relationship between *Kp* Mag and noise for the *Kepler* detector with high pointing precision, with the median represented by the larger green circles outlined in black. Each blue point is a simulated light curve with no motion vectors injected into the centroid position of the PSF. The primary contributors to this trend are photon noise and background noise, which were calibrated in our simulation by matching the slope of the *Kepler* trend.
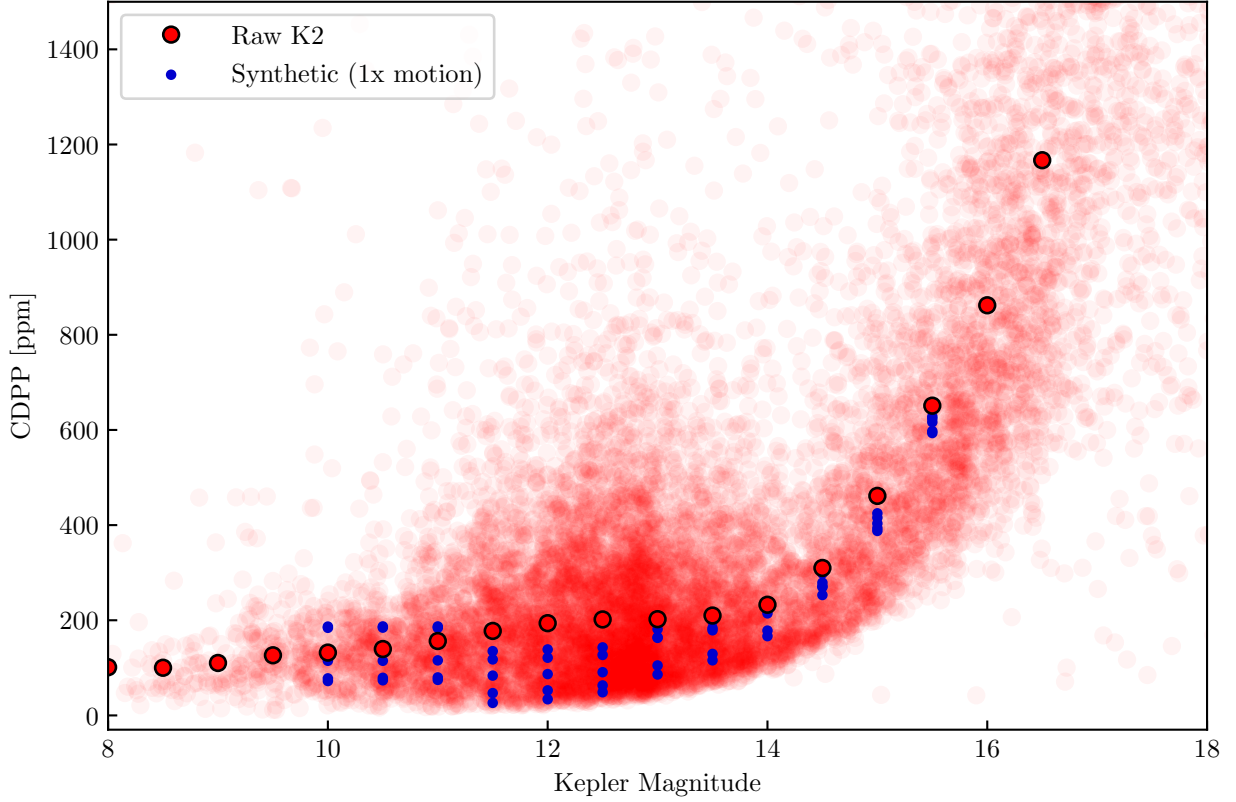
Fig. 2.— Benchmark Test 2: Noise level (CDPP) of our simulated light curves with *K2* motion compared to real *K2* targets as a function of *Kp* Mag. The points displayed in red show the noise of 1,000 raw *K2* observations before de-trending with the EVEREST pipeline, and the larger red points outlined in black follow the median of the trend. Each blue point is a simulated target with current *K2* motion and randomly varied initial centroid position and PSF shape. Our simulated data follow the same CDPP vs. *Kp* Mag relationship as real data, indicating that the sensitivity variation in our model appropriately captures the detector.
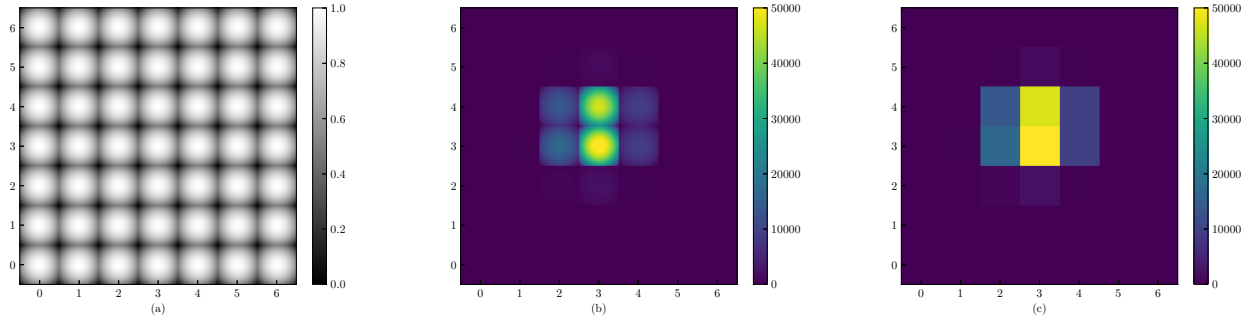
Fig. 3.— (a) A sample detector with sensitivity variation and no stellar targets, where white represents 100% photon detection efficiency, and the shaded regions have lower values for quantum sensitivity. Note that our model peaks in sensitivity at the center of each pixel and falls off towards the edges. There is also slight random variation in sensitivity between pixels. (b) A Stellar PSF projected onto the detector at the sub-pixel level. The sensitivity variation has been exaggerated in this simulation to demonstrate the variation in sub-pixel fluxes. (c) The final interpolated image. The value of each pixel is the integral over x and y of the sub-pixel flux.
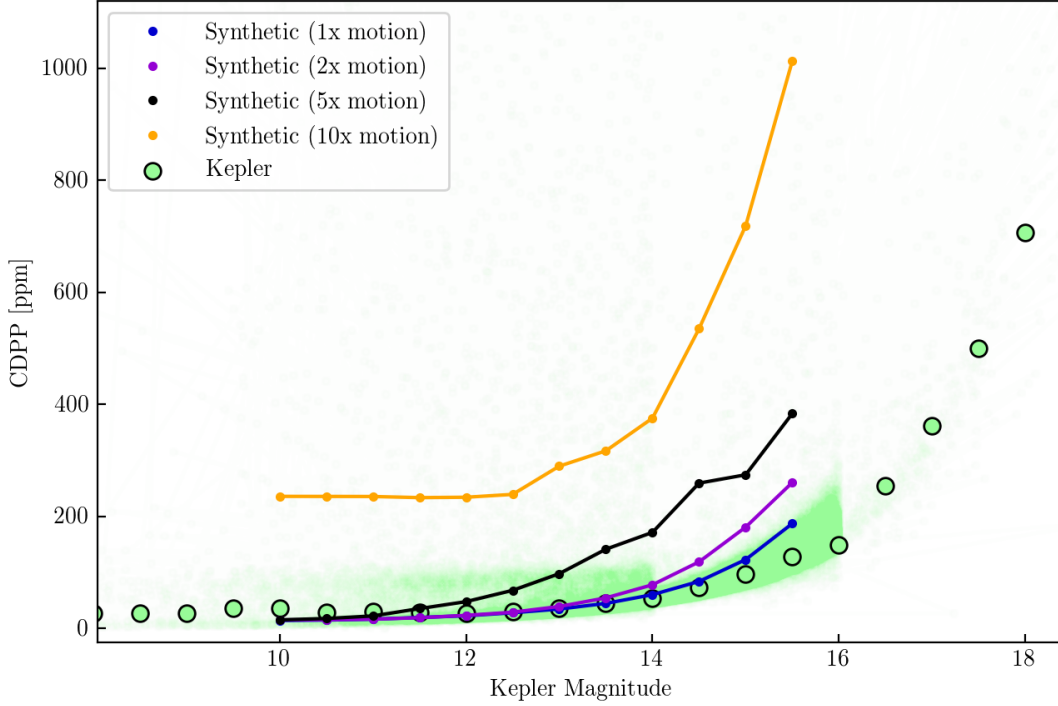
Fig. 4.— Noise level (CDPP) of simulated light curves after de-trending with 2nd order Pixel Level Decorrelation (PLD) as a function of Kp Mag. The green points show noise levels of 1,000 targets from the original *Kepler* mission with the median represented by the larger green circles outlined in black. De-trended simulated light curves with 1x, 2x, 4x, and 10x current *K2* motion are represented by the solid trends, and each point is the mean of 5 simulated light curves of a given Kp Mag with slightly varied PSF shape and initial centroid positions. We achieve sub-400 ppm CDPP up to 5x motion for targets up to Kp Mag = 15.5, and de-trended light curves up to 10x motion perform better that group based observation (for which $< 1,000$ ppm is difficult to achieve).

REFERENCES

Aigrain, S., Hodgkin, S. T., Irwin, M. J., Lewis, J. R., & Roberts, S. J. 2015, MNRAS, 447, 2880

Aigrain, S., Parviainen, H., & Pope, B. J. S. 2016, MNRAS, 459, 2408

Armstrong, D. J., Kirk, J., Lam, K. W. F., et al. 2015, A&A, 579, A19

Deming, D., Knutson, H., Kammer, J., et al. 2015, The Astrophysical Journal, 805, 132. http://stacks.iop.org/0004-637X/805/i=2/a=132

Howell, S. B., Sobeck, C., Haas, M., et al. 2014, PASP, 126, 398

Huang, C. X., Penev, K., Hartman, J. D., et al. 2015, MNRAS, 454, 4159

Luger, R., Agol, E., Kruse, E., et al. 2016, AJ, 152, 100

Luger, R., Kruse, E., Foreman-Mackey, D., Agol, E., & Saunders, N. 2017, ArXiv e-prints, arXiv:1702.05488

Lund, M. N., Handberg, R., Davies, G. R., Chaplin, W. J., & Jones, C. D. 2015, The Astrophysical Journal, 806, 30. http://stacks.iop.org/0004-637X/806/i=1/a=30

Van Cleve, J. E., & Caldwell, D. A. 2016, doi:KSCI-19033-002

Vanderburg, A., & Johnson, J. A. 2014, PASP, 126, 948

Vorobiev, D., Ninkov, Z., Caldwell, D., & Mochnacki, S. 2018, ArXiv e-prints, arXiv:1806.07430